Received: 21 July 2021 | Revised: 15 July 2022 | Accepted: 21 July 2022

DOI: 10.1002/hyp.14673

RESEARCH ARTICLE

WILEY

Analysing the capability of a catchment's spectral signature to regionalize hydrological parameters

Laura Fragoso-Campón[1] | Pablo Durán-Barroso[2] | Elia Quirós[1]

[1]Department of Graphic Expression, Universidad de Extremadura, Cáceres, Spain

[2]Department of Construction, Universidad de Extremadura, Cáceres, Spain

Correspondence
Laura Fragoso-Campón, Universidad de Extremadura, Escuela Politécnica, Avda. de la Universidad s/n, Cáceres 10003, Spain.
Email: laurafragoso@unex.es

Funding information
Consejería de Economía, Ciencia y Agenda Digital de la Junta de Extremadura; European Regional Development Fund, Grant/Award Numbers: GR18028, GR18052; European Social Fund, Grant/Award Number: PD16018; Universidad de Extremadura, Grant/Award Number: 2021-1852X2-CONVENIO 025Ñ16

Abstract

Water resource management in ungauged catchments is complex due to uncertainties around the hydrological parameters that characterize streamflow behaviour. These parameters are usually defined by regionalization approaches, in which the hydrological response patterns of ungauged basins are inferred from those of gauged basins. Regression-based methods using physical properties derived from cartographic data sources are widely used. The current remote sensing techniques offer new opportunities for the regionalization of hydrological parameters since the hydrological response depends on the physical attributes related to the spectral responses of a given land surface. Moreover, machine learning approaches have not been specifically applied to the regionalization of hydrological parameters in forested areas. This work studies the capability of a catchment's spectral signature based on Sentinel-1 and Sentinel-2 data to address a regression-based regionalization of hydrological model parameters using a machine learning approach. Hydrological modelling was conducted by the HBV-light model. We tested the random forest algorithm in several regionalization scenarios: the new approach using the catchments' spectral signature, the traditional method using physical properties and a fusion of these methods. The calibration results were excellent (median KGE = 0.83), and the regionalized parameters achieved good performance, in which the three scenarios showed almost the same goodness of fit (median KGE = 0.45–0.50). We found that the effectiveness depends on the climatic environment and that predictions in humid catchments exhibited better performance than those in the driest catchments. The physical approach (median KGE = 0.71) exhibited better performance than the spectral approach (median KGE = 0.64) in humid catchments, whereas spectral regionalization (median KGE = 0.33) enhanced the physical scenario in the driest catchments (median KGE = 0.25). Our results confirm that regionalization is still challenging in drier climates, such as in the Mediterranean environment. The new spectral approach showed promising results and it was effective in the analysis of the relationship between the spectral response of the territory and its hydrological characteristics, specially, where no cartographic data is available.

KEYWORDS
HBV, hydrology, random forest, runoff, SAR, sentinel

1 | INTRODUCTION

Water resource management requires accurate quantification of all hydrological processes involved in water supply, flood and drought evaluations and eco-hydrology (Cui et al., 2020; Hrachowitz et al., 2013). Hydrological modelling is complex and depends on the availability of input data and on the uncertainties of the parameters that must be calibrated to obtain good accuracy in streamflow simulations (Beck et al., 2020). Moreover, calibration can lead to nonunique combinations of best parameters (Bárdossy, 2007) and uncertainty in the quantification of actual hydrological processes is even greater in ungauged catchments, where calibration of model parameters is not feasible, thus presenting a challenge for hydrologists.

For ungauged catchments, the regionalization approach is used to infer hydrological response patterns from gauged catchments (Hrachowitz et al., 2013), and in recent decades, different regionalization methodologies have been proposed to better understand hydrological processes in ungauged areas. These methodologies are well documented in previous studies, such as the reviews by Hrachowitz et al. (2013), Parajka et al. (2013) and Guo et al. (2021). However, the regionalization of hydrological parameters in ungauged catchments remains a challenge. This challenge is evidenced by the fact that numerous studies have been published in the last years that analysed different regionalization approaches and it is not clear that there is one method that truly works better than others. Table 1 summarizes some of these studies, organized depending on the information to be transferred, whether hydrological model parameters or hydrological signatures, and according to different regionalization methodologies such as the categories proposed by Guo et al. (2021): similarity-based, regression-based, and hydrological signatures-based approaches.

Thus, as mentioned above, there is no optimal regionalization method and, as suggested by Parajka et al. (2013), the effectiveness of regionalization will depend on the environment and the particular hydroclimatic attributes of an area. In this regard, Yang et al. (2019) analysed which aspect of the prediction of future hydrological processes (regionalization methods or climate models) had more influence on the overall uncertainty and found that the main source of uncertainty depended on catchment attributes. Specifically, the regionalization method, rather than climate variables, tended to dominate the uncertainty in the lower precipitation areas of their study.

The present work focuses exclusively on parameter regionalization, analysing the relationships between catchment characteristics and the hydrological parameters that best represent the catchment hydrological response. Table SI.1 shows, to the best of our knowledge, the most recent studies specifically focused on parameter regionalization, summarizing the main characteristics of each study as well as the main results obtained.

Nevertheless, the transferability of parameters does not always lead to satisfactory simulation results due to nonlinear functions between the heterogeneous catchments and their flow regimen (Bárdossy, 2007). In the last decade, machine and deep learning methods have been proven to be effective in analysing nonlinear relationships in many geoscience areas, particularly in water science areas (see reviews by Tyralis et al. (2019) and Shen (2018)). However, only a few studies have used machine learning for the regionalization approach of streamflow simulations (Buzacott et al., 2019; Kult et al., 2014; Ma et al., 2021; Prieto Sierra et al., 2019; Snelder et al., 2009; Zhang et al., 2018), and to the best of our knowledge, there is a lack of studies applying machine learning algorithms specifically to the regionalization of hydrological parameters. To the best of our knowledge, only the study by Saadi et al. (2019) examined the potential of the random forest algorithm for regionalizing hydrological parameters in urban catchments, and the regionalized models achieved good performance.

With respect to the physical properties, topographic, land use, soil, and geological data from cartographic sources are traditionally the most used to characterize catchments for parameter regionalization (Booij, 2005; Hundecha & Bárdossy, 2004; Kult et al., 2014; Merz & Blöschl, 2004; Parajuli et al., 2018). Recent studies have incorporated remote sensing data as predictors, such as those of Choubin et al. (2019) who used Moderate Resolution Imaging Spectroradiometer (MODIS) images and some derived products, such as vegetation and biophysical indices, to estimate streamflow in ungauged catchments. Landsat-8-derived indices have been used for flood susceptibility mapping (Bui et al., 2020), and Beck et al. (2020) used the mean normalized difference vegetation index (NDVI) from the SPOT vegetation program as a predictor in their global regionalization of hydrological parameters. Finally, Jillo et al. (2017) also used the NDVI from the International Water Management Institute (IWMI) as a predictor in their regionalization of hydrological parameters in Ethiopia. However, apart from their use in vegetation indices, remote sensing data can also add a valuable characterization of catchments because the spectral response will depend on the vegetation (type and cover) and on the geological and lithological characteristics of the study area. Moreover, the vegetation types are also related to the soil lithotypes (Costa et al., 2017). Hence, the reflectance captured by the optical sensor is related to the surface mineralogy, depending on the composition of the soil of the geological formations of the area (Rajendran & Nasir, 2021). Moreover, the response of synthetic aperture radar (SAR) backscatter intensity is affected by surface roughness, soil moisture content (Purinton & Bookhagen, 2020), dielectric constant and grain size (Lu et al., 2021). Consequently, considering that the abovementioned characteristics are directly involved in the hydrological response of the territory, the spectral response of a catchment can be related to its hydrological behaviour. Thus, remote sensing data offer new opportunities to improve the prediction of hydrological processes in ungauged catchments. However, to our knowledge, the capability of the spectral signature to study catchment properties and to be

TABLE 1 Regionalization studies based on different methodologies depending on the information to be transferred

Methodology	Study	Information to be transferred	
		Model parameters	Hydrological signatures
Similarity-based	Arsenault and Brissette (2016)	x	
	Pagliero et al. (2019)		x
	Swain and Patra (2019)		x
	Tegegne and Kim (2018)	x	
	Zamoum and Souag-Gamane (2019)	x	
Regression-based	Beck et al. (2020)	x	
	Götzinger and Bárdossy (2007)	x	
	Hundecha and Bárdossy (2004)	x	
	Jillo et al. (2017)	x	
	Merz and Blöschl (2004)	x	
	Saadi et al. (2019)	x	
Hydrological signatures-based	Betterle et al. (2019)		x
	Chouaib et al. (2018)	x	
	Jayathilake and Smith (2019)		x

used as predictors in regression-based regionalization of hydrological parameters in Mediterranean environments has not yet been documented.

Therefore, the aim of our study was to explore the capability of a catchment's spectral response for a regression-based regionalization of hydrological parameters using a machine learning approach. The specific goals were (i) to test the random forest algorithm for the regression of the hydrological parameters based on the spectral signatures of the catchments using Sentinel satellites, (ii) to compare the accuracy of the spectral-based approach with the traditional physical-based regionalization approach, and (iii) to evaluate the contribution of the spectral-based regionalization approach to the better understanding of catchment hydrological response in ungauged catchments in the Mediterranean climatic environment.

2 | DATA AND METHODS

2.1 | Study area

The study area comprises 18 gauged watersheds throughout the Extremadura region in Spain (Figure 1). The criteria for the selection of the watersheds were based on the availability of gauging station data measuring an upstream area of less than 1000 km^2 of mainly forested cover and not controlled by the regulation of any dam or reservoir to study the natural regime of the rivers. Table 2 shows the main climatic characteristics of the watersheds (Rivas-Martinez & Rivas-Saenz, 1996-2019), where the annual mean temperature and the mean annual precipitation range from 10 to 17°C and from 446 to 1323 mm, respectively. Precipitation occurs mainly from October to April, while June, July and August represent the dry season, with no or almost no precipitation in most years.

Figure 2 shows a flowchart of the methodology followed in this study which will be presented in the following sections.

2.2 | Data preprocessing

2.2.1 | River discharge

The river discharge data were supplied by the Automatic Hydrological Information Systems (SAIH) of the hydrographic regions of *Tajo* and *Guadiana*, to which the watersheds belong, and which have had data recorded since they were put into operation in 2008. Therefore, the daily discharge from January 2008 to December 2019 was analysed. To ensure the quality of discharge observations, the hydrograph was analysed by visual inspection to guarantee the absence of gaps and outliers. Since the natural regime of the rivers studied is intermittent, as recommended in Crochemore et al. (2020), it is important to distinguish between high-flow peaks instead of numerical outliers.

2.2.2 | Precipitation and temperature

In this work, the daily gridded dataset of temperatures (maximum and minimum) and 24 h accumulated precipitation developed by the Spanish Meteorological Agency (AEMET) available in AEMET (2019) was used. These gridded datasets were obtained through a statistical interpolation analysis of ground observation stations, with a spatial resolution of 0.05° in a rotated grid (CORDEX compliant) based on HIRLAM-AEMET Numerical Weather Prediction operational analyses (AEMET, 2017). To obtain the daily series in each watershed, we first reprojected the watershed into the rotated grid, and then, the average daily values in each watershed were processed.

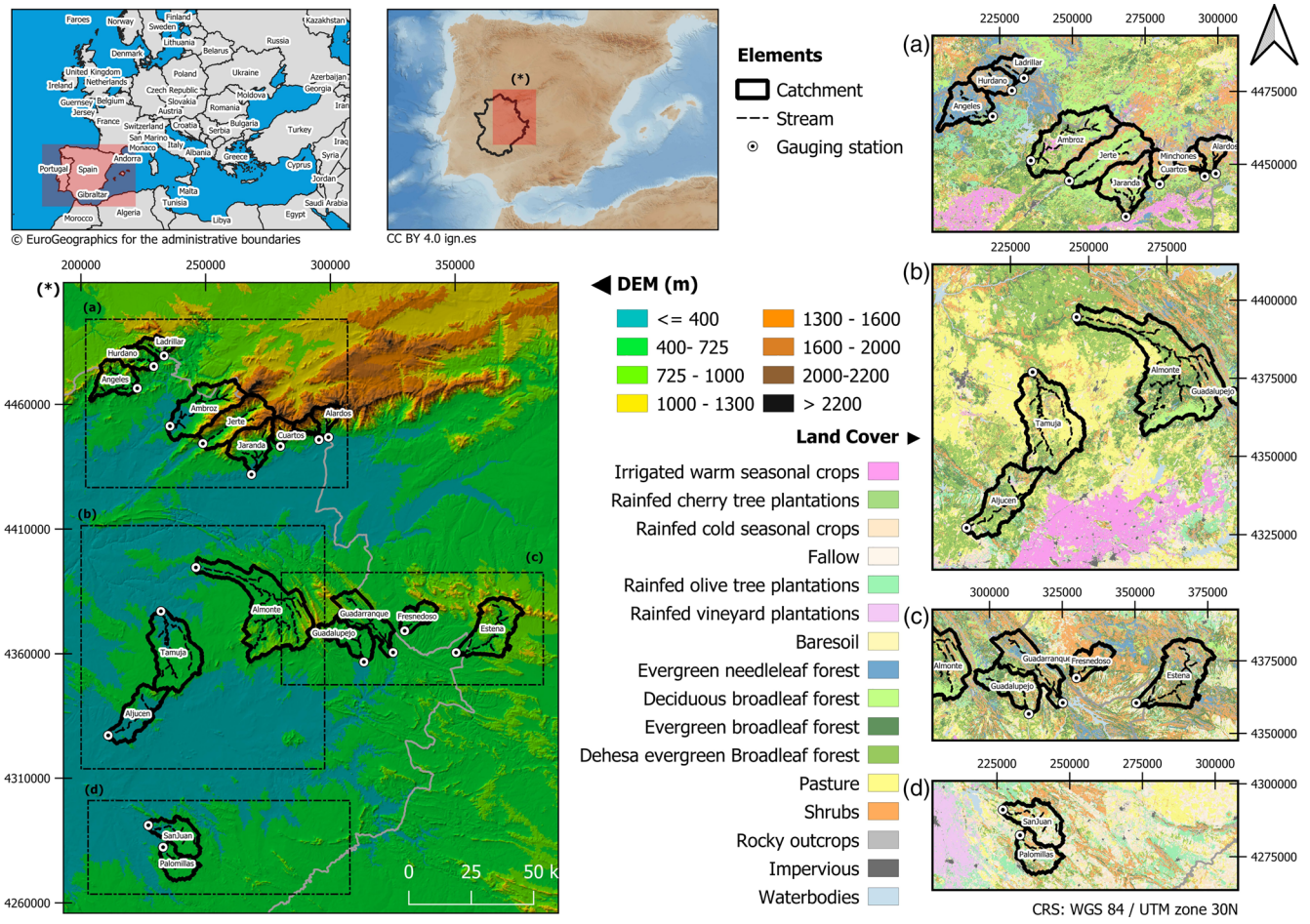

FIGURE 1 Location of the study area, DEM, and land cover

The main limitation of this dataset lies in the values of the interpolation at the highest elevation, where there are usually no ground observation stations and the values are interpolated from records of ground stations located, generally, at lower elevations. To address this issue, the hydrological model parameters related to the increase of precipitation with elevation (PCALT) and decrease of temperature with elevation (TCALT) were calibrated to ensure the balance of input and output volumes and minimize the error in volume. Then, for the regionalization stage, to analyse variations in temperature and precipitation with elevation in ungauged catchments, the differences in the elevation to the reference ground data and the mean distance to the nearest stations were analysed for each catchment.

2.2.3 | Potential evapotranspiration

The daily potential evapotranspiration was calculated using the 1985 Hargreaves ET_o equation since it only requires measured temperature data (see eq. 8 in Hargreaves et al. (2003)). The extraterrestrial radiation (R_a) values for the different latitudes of the watersheds were estimated following the equations in Allen et al. (1998). Finally, the long-term monthly mean values were obtained from the daily values of potential evapotranspiration from January 2008 to December 2019.

2.2.4 | Land cover and topographic data

The land cover map used in this work (Figure 1) was developed in a previous study in which hydrological land cover categories were mapped based on the runoff generation capability of the land cover types using remote sensing techniques (Fragoso-Campón, Quirós, & Gutiérrez Gallego, 2020). The land cover can be divided into three groups: forested, agricultural and impervious cover. Forested land cover categories comprise evergreen forest, deciduous forest, *dehesas*, shrubs, and herbaceous vegetation. The *dehesa* is a typical cover from Extremadura (Fragoso-Campón, Quirós, & Gutiérrez Gallego, 2020), defined by Devesa Alcaraz (1995) as '*pasturelands populated by holm and/or cork oaks, with an understorey of open grassland, cereal crops, or Mediterranean scrub*'. The agricultural land cover categories are rainfed crops (mainly olive trees, vineyards and cold-season annual crops and cherry trees) and irrigated crops (seasonal warm crops). Finally, impervious surfaces included rocky outcrops, bare soil, roads, and urban areas.

TABLE 2 Characteristics of the catchments

Catchments	Hydrographic region	Bioclimate variant[a]	*T* mean (°C)	*P* mean (mm)	Area (km^2)	Elevation (m)	LFP[b] (km)
Alardos	Tajo	Tocsm	10.36	1024.74	87.81	1287.34	18.85
Aljucén	Guadiana	Mpc	16.91	551.32	253.57	397.83	42.78
Almonte	Tajo	Mpc	15.59	736.99	781.36	639.62	92.96
Ambroz	Tajo	Tocsm	13.85	1104.15	390.49	760.47	47.68
Ángeles	Tajo	Tocsm	13.67	999.29	188.79	788.61	33.50
Cuartos	Tajo	Tocsm	10.52	1271.11	68.41	1259.59	17.31
Estena	Guadiana	Mpc	15.08	628.31	355.97	788.60	51.54
Fresnedoso	Guadiana	Mpc	15.61	579.58	107.07	642.07	22.80
Guadalupejo	Guadiana	Mpc	15.76	718.10	199.13	580.41	34.17
Guadarranque	Guadiana	Mpc	15.32	698.52	256.56	670.97	43.49
Hurdano	Tajo	Tocsm	13.16	974.48	108.58	852.21	31.69
Jaranda	Tajo	Tocsm	13.80	1243.26	225.29	815.32	30.88
Jerte	Tajo	Tocsm	11.57	1322.85	315.08	1131.62	42.76
Ladrillar	Tajo	Tocsm	12.89	980.22	73.11	890.68	17.09
Minchones	Tajo	Tocsm	11.10	1112.70	56.41	1305.55	15.19
Palomillas	Guadiana	Mpc	16.55	446.02	145.84	494.39	22.84
San Juan	Guadiana	Mpc	16.76	453.55	194.05	451.80	37.14
Tamuja	Tajo	Mpc	16.52	550.18	458.12	447.49	62.00

[a]Mediterranean pluviseasonal-continental (Mpc) and temperate oceanic sub-Mediterranean (Tocsm) by Rivas-Martinez and Rivas-Saenz (1996-2019).
[b]Longest flow path (LFP).

Digital elevation models (DEMs) at a spatial resolution of 25 m developed by the Spanish National Geographic Institute (IGN, 2021) were used for topographic data. Table SI.2 shows the properties considered as predictors in this study.

2.2.5 | Soil data

The spatial distribution of soil characteristics was obtained from the European Soil Data Centre (Joint Research Centre, 2020). Here, two different sources were used: we considered the information in the European Soil Database v2.0 (Panagos, 2006) for the characterization of the deeper groundwater response, whereas the updated topsoil and the physical properties for Europe developed in Ballabio et al. (2016) were used for the shallow groundwater response. Table SI.2 shows the physical soil properties considered as predictors in this study.

2.2.6 | Sentinel data

The spectral response of the catchments was studied using images collected from the Sentinel-1 (S1) and Sentinel-2 (S2) missions of the Copernicus Program. S1 is a C-band SAR sensor with dual VV and VH polarization, and S2 is a multispectral sensor working in the visible (VIS), near-infrared (NIR) and shortwave infrared (SWIR) bands. The analysis was addressed in multidate format: one S2 image acquired in summer when the soil and vegetation show the best spectral separability in the Mediterranean environment (Fragoso-Campón, Quirós, Mora, et al., 2020; Godinho et al., 2017) and two S1 images, one acquired in summer close to the S2 acquisition date and another S1 image in winter to capture seasonal phenological differences. The satellite images were preprocessed using Sentinel Application Platform (SNAP) software developed by the European Space Agency (ESA, 2019). S1 scene preprocessing included calibration (radiometric normalization), terrain correction and speckle filtering. S2 preprocessing included resampling, reprojection and mosaic building (further information is presented in Fragoso-Campón et al. (2021)). In addition, for a better characterization of the watersheds, spectral-derived metrics (vegetation, water, and soil indices) and texture metrics derived from the grey-level cooccurrence matrix (GLCM) were also used (Haralick & Shanmugam, 1973). These metrics have been proven to be very useful in previous works related to land cover (Fragoso-Campón et al., 2021) and lithological analysis (Lu et al., 2021; Radford et al., 2018). A complete description of these metrics is shown in Table SI.2.

2.3 | Hydrological model

2.3.1 | Model description

Herein, hydrological modelling was conducted by a conceptual-continuous rainfall-runoff model at the catchment scale using the HBV-light version of the HBV model (Bergström, 1995) developed by Seibert and Vis (2012). The model includes different routines (snow, soil, groundwater, and routing) and simulates catchment discharge based on time series of precipitation, temperature and potential

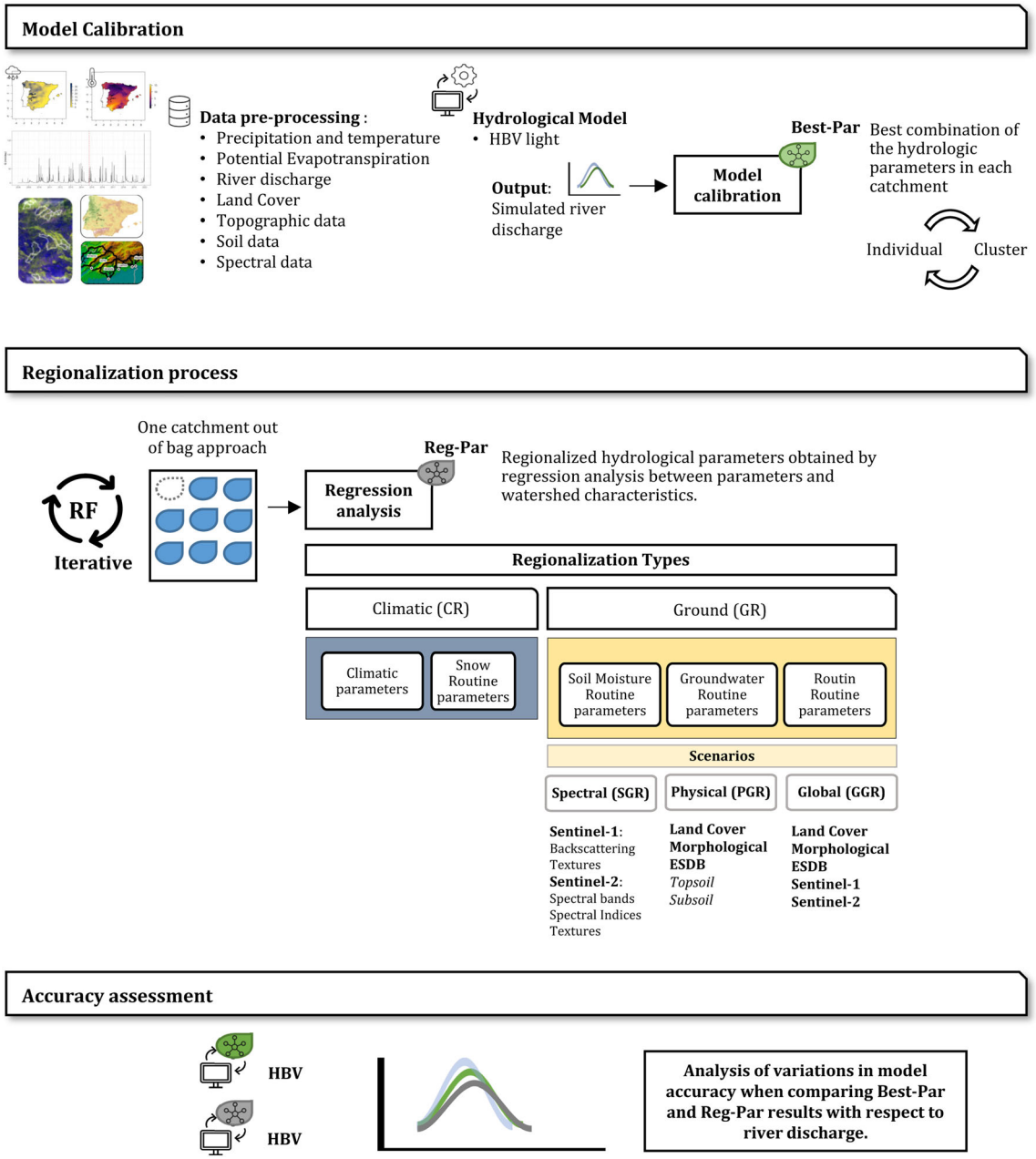

FIGURE 2 Processing flowchart of the methodology proposed in this study

evaporation data (a detailed description of the software and formulation is included in Seibert and Vis (2012)). We studied discharge at a daily time step for 11 years, dividing the time series into two periods: warm-up (January 2008–September 2014) and simulation (October 2014–December 2019).

The watersheds were analysed with a semidistributed approach by considering four elevation zones (counting the quantile distribution of the DEM) and three vegetation classes. The vegetation categories were grouped according to their runoff capability (low-medium-high): vegetation type 1 (low) comprises evergreen forest, deciduous forest, *dehesas*, and shrubs; vegetation type 2 (medium) comprises herbaceous vegetation and agricultural land cover; and vegetation type 3 (high) comprises impervious surfaces.

We used a model structure of three groundwater (GW) boxes: storage in the soil top zone (STZ), storage in the soil upper zone (SUZ) and storage in the soil lower zone (SLZ). Both the STZ and SUZ boxes are distributed using a box for each elevation-vegetation unit (Figure 3). The parameters involved in the model are related to each routine, as shown in Table 3.

2.3.2 | Model accuracy evaluation

The accuracy evaluation of the models was performed following the goodness-of-fit (GoF) functions implemented in HBV-light and also using a self-defined goodness of fit measure called Objective (Obj)

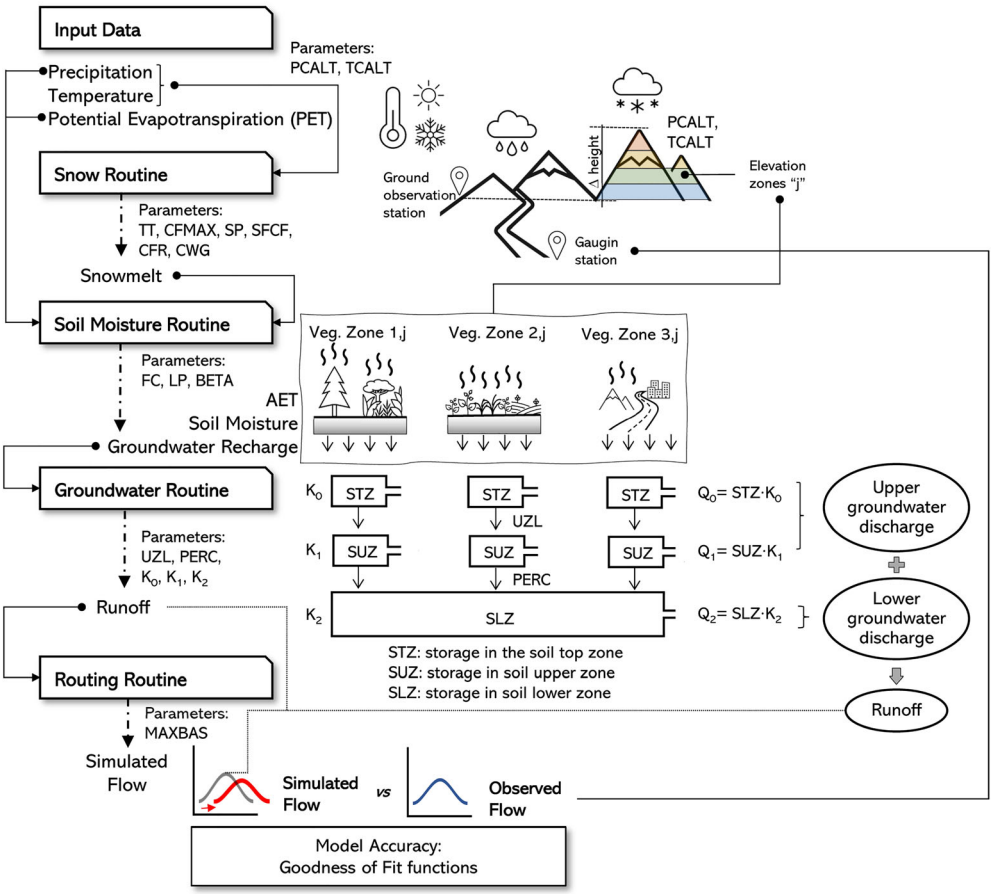

FIGURE 3 Schematic structure of the HBV-light model used in this study

function, using Reff, KGE, and Reff Peak, with weight values of 0.2, 0.6, and 0.2, respectively (see Table SI.3).

2.3.3 | Model calibration

The calibration of the model at the gauged basins was performed using a sequential regression approach (He et al., 2011) in two stages: the individual catchment approach and the cluster of catchments approach.

In the first stage, each catchment was examined individually to obtain the best combination of parameters in each catchment using the tools available in the HBV-light software: Monte Carlo simulations and genetic algorithm and Powell optimization (GAP). First, a Monte Carlo simulation of 50 000 runs was carried out. In each run, the parameter values were randomly chosen within the given range (Table 3), ensuring the lack of bias in the calibration procedure (Seibert, 1999). Then, the results were analysed to set the optimum range of PCALT and TCALT parameters to minimize the water balance volume error. Then, another 50 000 Monte Carlo simulations were run, and the simulation results were analysed considering the GoF function results for each parameter, defining the optimum range to maximize the accuracy of the model. The last step consisted of the application of the GAP algorithm within the optimal boundaries of the parameters obtained in the previous steps, and as a result, the parameters were fine-tuned using Powell's quadratically convergent method as described in Seibert and Vis (2012). The best parameter value combination was calculated for an objective function using Reff, KGE, and Reff Peak, with weight values of 0.2, 0.6, and 0.2, respectively.

In the second stage, the best values were analysed from the cluster criteria point of view, applying a physical similarity-based approach prior to the regression analysis itself. As mentioned in previous studies, calibration could lead to a nonunique combination of best parameters (Bárdossy, 2007; Hundecha & Bárdossy, 2004), since different combinations of values can lead to the same efficiency. In this study it is assumed that the hydrological response in watersheds with similar characteristics is meant to be similar, so the values of the parameters of the hydrological model should also be similar. To do this, we conducted a cluster analysis, which grouped the watersheds that were maximally similar with respect to their characteristics. Once the basins have been grouped, the values obtained for each parameter were analysed within the cluster and, if necessary, parameters outside of the cluster trend were revaluated using the GAP algorithm using as limit values those defined as non-outliers in the cluster trend.

Cluster analysis was performed using the Ward hierarchical clustering method (Ward, 1963) with Euclidean distances implemented in R Stats Package R Software (R-Core-Team, 2018). This cluster analysis grouped the watersheds that were maximally similar with respect to their characteristics considering the physical and spectral information proposed in this work. Formerly, for the cluster analysis, the parameters

TABLE 3 List of parameters involved in each HBV-light routine

Model routine	Input data	Parameters	Description	Unit	Range	Output data
-	Precipitation (Pi)	PCALT	Increase of precipitation with height increment	%/100 m	10–30	*P*
-	Temperature (Ti)	TCALT	Decrease of temperature with height increment	°C/100 m	0.6–1	*T*
-	Potential evapotranspiration (PET)	-	-	mm/Δt	-	PET
Snow routine	*P* and *T*	TT	Threshold temperature at which the accumulation of precipitation is in the form of snow below it	°C	−2 to 0.5	Snowmelt
		CFMAX	Degree-Δt factor for snow melting that starts if temperatures are above TT	mm °C^{-1} Δt^{-1}	0.5–4	
		SP	Seasonal variability in degree-Δt factor	-	0	
		SFCF	Snowfall correction factor	-	0.5–0.9	
		CFR	Refreezing coefficient	-	0.05	
		CWH	Water holding capacity of melted water that refreezes again when temperature decrease below TT	-	0.01	
Soil moisture routine	*P*, snowmelt and PET	FC	Maximum soil moisture storage	mm	50–550	AET, soil moisture and groundwater recharge
		LP	Soil moisture value above which actual evapotranspiration (AET) reaches PET	mm	0.3–1	
		BETA	Parameter that determines the relative contribution to runoff from rain or snowmelt	-	1–5	
Groundwater routine	Groundwater recharge and PET	UZL	Maximum percolation from the STZ to the SUZ	mm	0–70	Runoff
		K_0	Recession coefficient of STZ	Δt^{-1}	0.1–0.5	
		K_1	Recession coefficient of SUZ	Δt^{-1}	0.01–0.2	
		K_2	Recession coefficient of SLZ	Δt^{-1}	0.00005–0.1	
		PERC	Maximum percolation from the SUZ to the SLZ	mm Δt^{-1}	0–4	
Routing routine	Runoff	MAXBAX	Length of triangular weighting function	Δt	1–2.5	Simulated runoff

were scaled with a centring approach (subtracting the mean and dividing by the standard deviation). As a result, the best combination of the parameters in each catchment was established (Best-Par).

In addition, an evaluation of the parameter sensitivity was assessed in each catchment using a Monte Carlo simulation of 10 000 runs, one simulation per parameter, using the Best-Par combination, varying one parameter per simulation and measuring the decrease in accuracy when changing the parameter value within the original range (Table 3). Hence, to analyse how well the models fit the best value of the calibration (target value), the objective GoF values were calculated in each run and the ratio to the target value was computed. Thus, a ratio of approximately 1 implies that the GoF value of the objective function is as good as the results obtained by the Best-Par algorithm and that the accuracy of the model is less sensitive to the parameter value. For all the runs, the minimum, mean, median and maximum values of the ratio were calculated for each parameter.

2.4 | Regionalization process

The regionalization process relies on the hypothesis that the hydrological response in watersheds with similar characteristics is meant to be similar. Therefore, once the Best-Par combination was obtained in each catchment, the next step was to establish the relationship of those parameters to the catchment characterization by training the machine learning algorithm used for the regression analysis. In this work, we addressed the regionalization analysis considering two point of views: on the one hand, the variables related to precipitation, temperature and snow routine, referred to as climatic regionalization (CR), were based on the topographic situation and climatology, and, on the other hand, the parameters involved in soil, groundwater and routing routines, referred to as ground regionalization (GR), depended on the catchment's properties in terms of spectral profile, morphology, land cover and soil characteristics. In addition, for the GR, we considered

TABLE 4 Types of regionalization and scenarios considered

Regionalization	Code (scenarios) and description		
Climatic	CR	Regionalization of parameters related to precipitation, temperature and snow routines	
Ground	GR	Regionalization of parameters involved in soil, groundwater and routing routines	
	(Physical)	PGR	The attributes of the watersheds are based on the cartographic data of vegetation cover, morphological information, and the soil (topsoil and subsoil) characterization of the European Soil Data Centre
	(Spectral)	SGR	The attributes of the watersheds are based on the spectral signature obtained from the Sentinel satellites
	(Global)	GGR	The attributes are a data fusion of the cartographic and spectral signatures

three scenarios to characterize the catchment properties, as shown in Table 4: spectral ground regionalization (SGR), physical ground regionalization (PGR) and global ground regionalization (GGR). The complete description of the predictors used for the regression is provided as supporting information in Table SI.2.

The regression analysis between parameters and characteristics in each scenario was conducted with the random forest (RF) algorithm (Breiman, 2001), which is a nonparametric machine learning method that has been proven effective for working with mixed-origin-input predictors such as those used in this work. Here, the regressions were performed using the RandomForest R package (Liaw & Wiener, 2002) with a number of decision trees (Ntree) of 5000. The number of variables to be selected when growing the trees (Mtry) was automatically trained by the algorithm for each scenario depending on the number of predictors in each scenario.

Due to the limited number of watersheds, we conducted an iterative regression adjustment with a one catchment out of bag approach, which consists of leaving out of the algorithm the characteristics of one of the catchments and running the RF algorithm to calculate the regionalized parameters (Reg-Par) considering the data of the other catchments. After the 18 RF simulations, all the Reg-Pars were compared to the Best-Par, and the RMSE was calculated for each parameter. Finally, the accuracy assessment of the regionalization in the different scenarios was addressed by running the HBV model using the Reg-Par obtained for each catchment and analysing the variations in the GoF functions when compared to the results of the Best-Par. This point was addressed separately for each scenario, CR and GR, and the assessment of the decrease in accuracy with respect to the calibration values for each one, was carried out using the Best-Par values of the parameters of complementary routines, Best-Par values of GR parameters when evaluating the efficiency of CR and vice versa.

3 | RESULTS

3.1 | Model calibration results

After the calibration process, the Best-Par combination was obtained for each catchment, and the main statistics are shown for each cluster as supporting information in Table SI.4. Figure 4 shows the spectral and physical density profiles of the catchments categorized into groups that are maximally similar with respect to their properties based on the dendrogram of the clustering analysis. It should be noted that the clusters, were in accordance with the different bioclimatic variants existing in the study area (Table 2), with groups 1 and 5 corresponding to the Mpc variant, the driest, and groups 2, 3, and 4 to the Tocsm variant, the wettest.

The accuracies of the models were excellent as shown in Table 5, where the global median objective GoF function value was 0.73. The best performing clusters are numbers 2, 3, and 4, which perform better than the global mean value, while clusters 1 and 5 are slightly lower but still outstanding.

The sensitivity analysis of the parameters measured how well the models fitted to the objective target value in each catchment for the Monte Carlo simulation of 10 000 runs. Therefore, values of adjustment of approximately 1 imply that the GoF is as good as the results achieved by Best-Par, so that the model is less sensitive to the parameter value.

Evaluating all the catchments together, the results showed that the model accuracy was most sensitive to variations in FC, UZL, and K0. In addition, differences in the sensitivity among the catchment clusters were observed and also considering the bioclimatic variants (Figure 5). In this sense, cluster 1 and cluster 5, both corresponding to the Mpc variant, showed the highest sensitivity to BETA, FC, and UZL, while in all three clusters belonging to the Tocsm variant, the most sensitive parameters were found to be PCALT and TCALT and FC, UZL, and K0. Specifically, cluster 3 showed high sensitivity to FC and PCALT and the lowest sensitivities appeared for cluster 2 and cluster 4, which were sensitive to K0, PCALT, and TCALT and to FC, UZL, and K0, respectively.

3.2 | Regionalization results

3.2.1 | Random forest regressions

The regression analysis was conducted with the RF algorithm in an iterative regression adjustment with one catchment out of bag at a time. The CR Reg-Par fit well to the Best-Par values, achieving good correlations and reasonable RMSE. The GR achieved almost the same

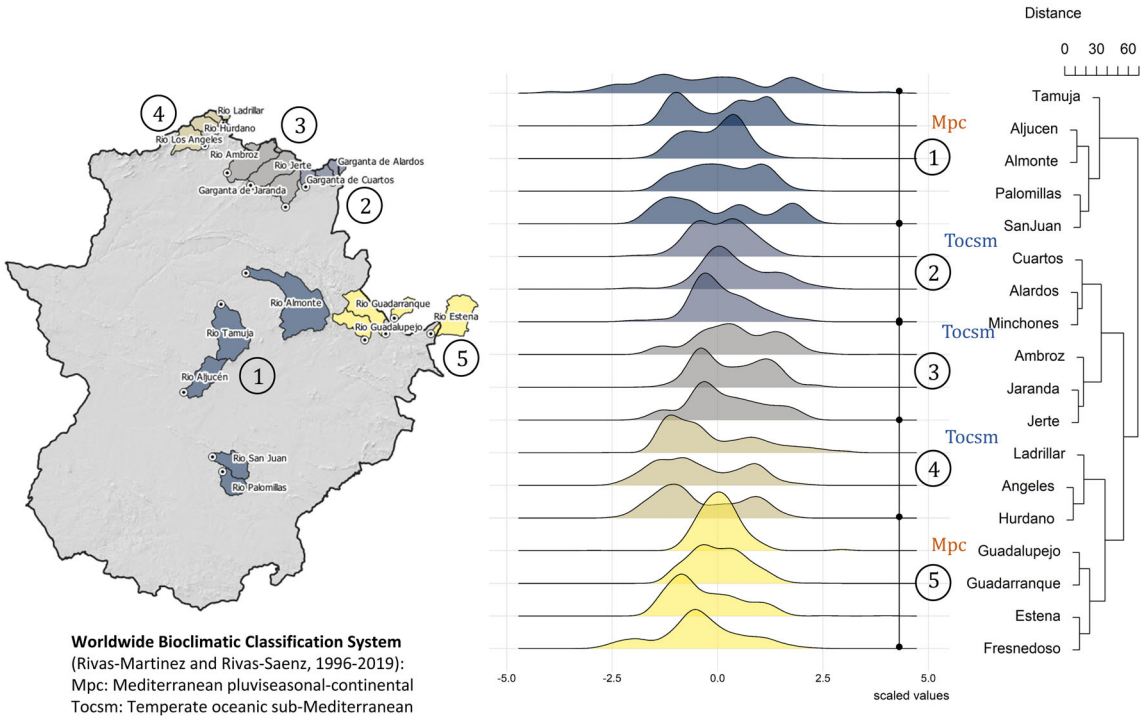

FIGURE 4 Catchment's spectral and physical density profile and clustering dendrogram based on the Ward error sum of squares hierarchical clustering method with Euclidean distances

TABLE 5 Median values in each GoF function obtained in the evaluation of the catchments globally and grouped by clusters

GoF function	Global	Cluster 1	Cluster 2	Cluster 3	Cluster 4	Cluster 5
Coefficient of determination	0.71	0.63	0.73	0.83	0.69	0.69
Model efficiency	0.68	0.63	0.72	0.79	0.68	0.67
Kling-Gupta efficiency	0.83	0.78	0.84	0.86	0.81	0.81
Efficiency for log(Q)	−0.36	−0.51	−0.29	0.65	0.30	−0.97
Flow weighted efficiency	0.83	0.72	0.86	0.90	0.71	0.84
Efficiency for peak flows	0.52	0.49	0.73	0.81	0.61	0.32
Volume error	0.98	0.98	0.99	0.98	0.97	0.98
Objective	0.73	0.69	0.79	0.83	0.74	0.68

performance in the three scenarios, where PGR achieved slightly better results in terms of both RMSE and Pearson correlation coefficient. The RMSE values between Reg-Par and Best-Par are shown as supporting information in Table SI.5, and Figure 6 shows the correlation in the most sensitive parameters of the model.

The importance of each predictor in the regression algorithms was analysed in terms of the increase in the mean squared error when a predictor is randomly permuted (%IncMSE), and higher values suggest a more important role of the predictor in the regression (Figure SI.1). In the CR, the most influential predictor is a topographic measurement referring to differences in the height of the catchments to the ground-observation digital elevation model (Delta_sd) and the climatic variables (*T*_mean and *P*_mean). In the SGR, the more valuable predictors are mainly related to texture metrics (for both SAR and optical bands) and the blue and NIR bands, and VIs such as MSAVI2 and SAVI seem to have a high influence on the prediction. In the PGR, topsoil properties are the most valuable predictors together with vegetation coverage. When all the GR predictors are combined in the GGR, the topsoil attributes remain valuable predictors, together with the texture-derived metrics from the SAR and NIR bands.

3.2.2 | Accuracy assessment of model predictions

Figure SI.2 shows the accuracy assessment of models in the different regionalization scenarios when Reg-Par was used compared to the results for Best-Par in each catchment, where the value for a perfect fit is 1, and values below 0 indicate poor fit.

Figure 7 represents the boxplot graphic of the GoF function values in both bioclimatic variants in the study area. The general

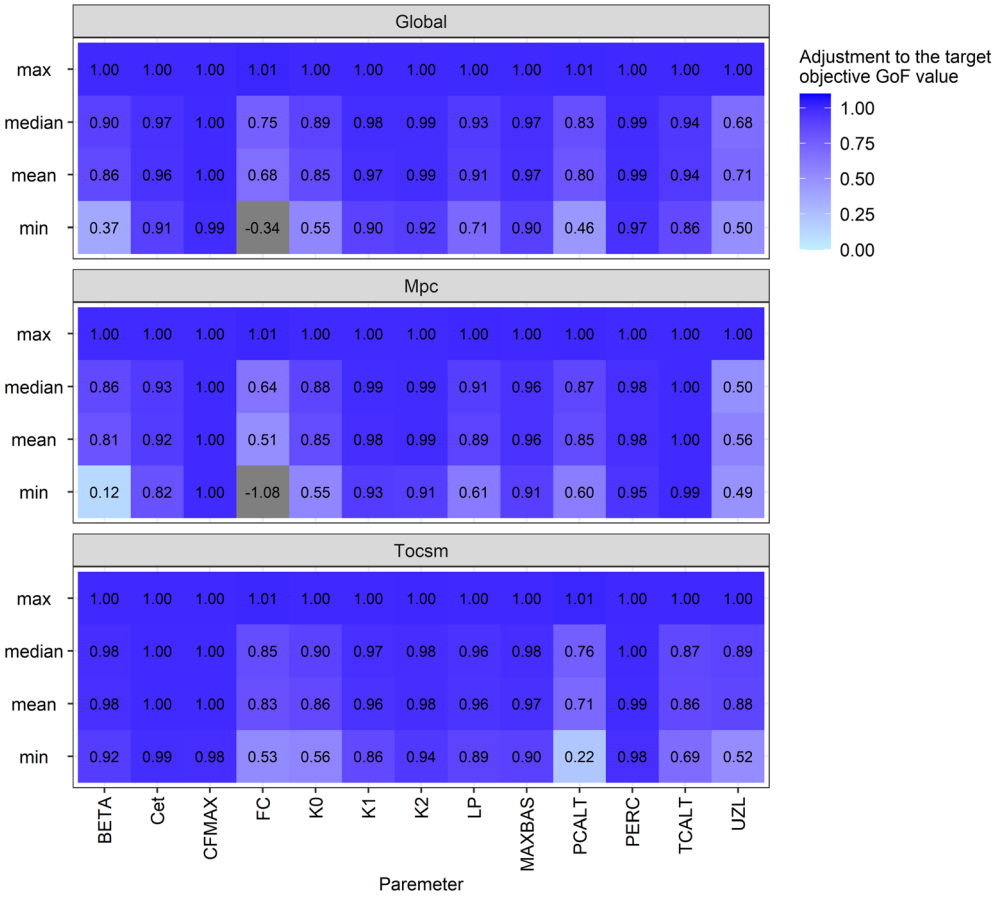

FIGURE 5 Results of the sensitivity analysis. Values of adjustment of approximately 1 imply that the GoF value is as good as the results achieved by the Best-Par algorithm and that the accuracy of the model is less sensitive to the value of the parameter

trend, when considering both bioclimatic variants together, was that the decrease in the GoF functions relative to the calibration values was less for the CR than for the GR, and the three scenarios in the GR achieved almost the same performance. The CR & GGR scenario achieved slightly lower accuracies. Against the general trend, the efficiency for log(Q) was highly improved in all GR scenarios. Regarding the differences among the groups, clusters 2 and 4 showed the best performance in the regionalization validation, whereas cluster 5 achieved the lowest accuracies. The SGR results were better in clusters 1, 3, and 5, followed by the PGR scenario. The GoF function with the greatest differences is Reff Peak, mostly in clusters 1 and 5. More detailed results of the variations in the GoF measurements in the scenarios for all the catchments and the behaviours grouped by clusters are included in Figure SI.3.

Finally, an example of observed and simulated streamflows in the scenarios are graphically presented in Figure 8 for the Angeles catchment.

4 | DISCUSSION

In this study, the capability of a catchment's spectral signature to aid in regionalizing hydrological parameters was analysed using a regression-based machine learning approach using random forest algorithm. The evaluation of the overall efficiency using the most common GoF functions showed very good performance in the calibration stage (Table 5) and was still outstanding in the regionalization results (Figure 7). Notably, the lack of previous studies at similar latitudes and in other Mediterranean climate variants hinders the comparison of the effectiveness of our work; consequently, we compared our results with previous studies using any regionalization approach. To this end, our results are briefly summarized in Table 6 and contrasted with the results of noted previous studies in terms of the median overall KGE and Reff values, the latter also referred to as Nash-Sutcliffe efficiency (NSE).

4.1 | Calibration performance

Concerning our calibration results, referring to the validation period, our findings, in both GoF terms, outperformed those reported in previous works, such as those shown in Table 6. Regarding KGE, our results are better than those reported by Jillo et al. (2017) and those reported by Beck et al. (2020), especially when compared with the results referred to for the arid climate group (visual interpretation of fig. 5 in their work). In addition, our results are similar to those reported by Alfieri et al. (2020) for Europe (visual interpretation of fig. 6 in their work). In terms of Reff, our results agreed with those reported by Merz and Blöschl (2004) and Jin et al. (2009). In addition, our results are better than those reported by Götzinger and Bárdossy (2007) and similar to those reported by Parajka et al. (2007) but lower than the results reported by Oudin et al. (2008). Notably, our

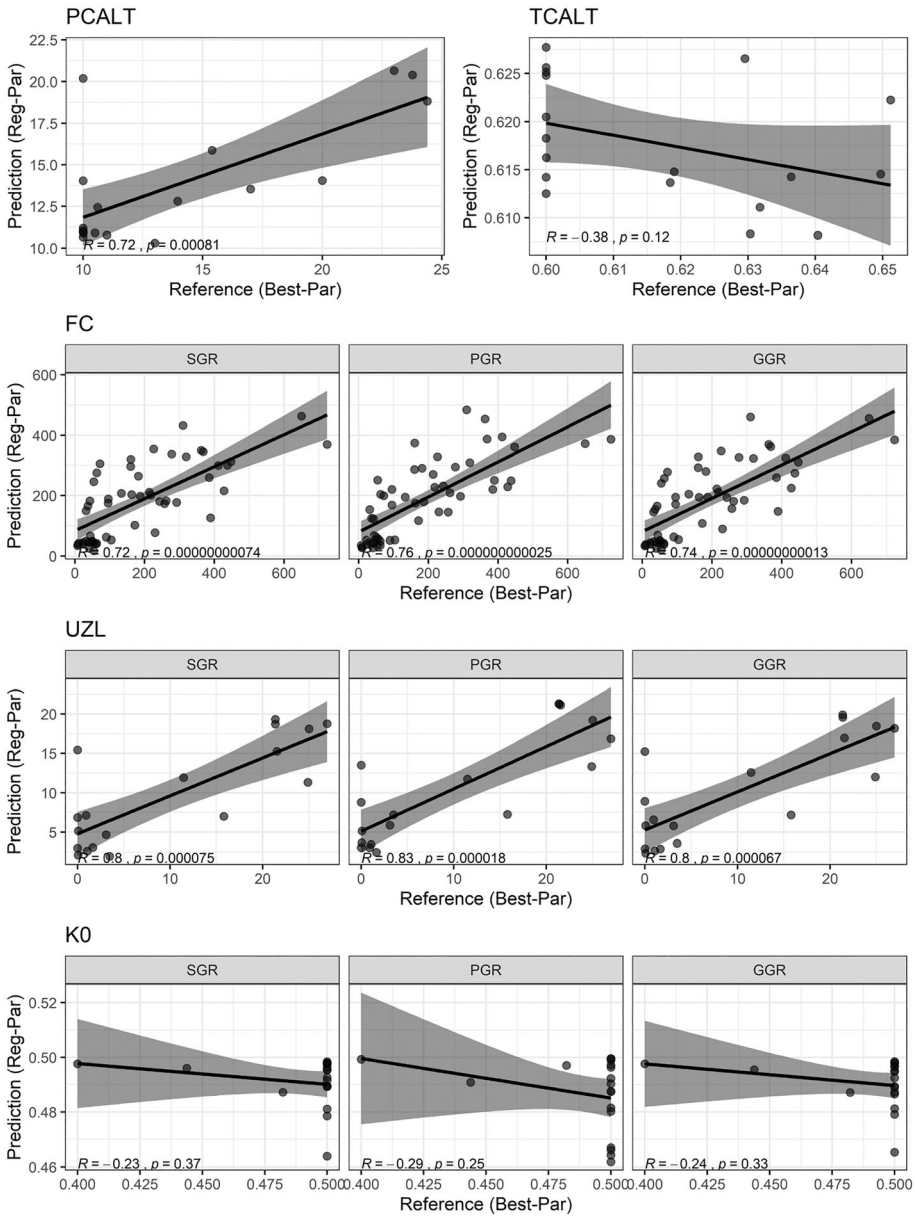

FIGURE 6 Scatter plots of the regionalization results of the most sensitive parameters of the models. *R* is the Pearson correlation coefficient, and *p* is the *p*-value

calibration was carried out based on the optimization of an objective function where Reff and KGE were weighted 0.20 and 0.60, respectively. We also considered Reff Peak weighted by 0.20.

4.2 | Regionalization performance

4.2.1 | Influence of climatic variants on the prediction of hydrological processes in ungauged catchments

The clustering analysis showed different efficiencies depending on the climatic point of view. In this sense, the prediction catchment classified as the Tocsm bioclimatic variant (clusters 2–4), the most humid variant, exhibited better performance than that classified as the Mpc bioclimatic variant (clusters 1 and 5), the driest variant, in both the calibration and regionalization stages (Figure 7). This finding agrees with the findings in the review by J Parajka et al. (2013), who indicated that the performance of runoff predictions tends to be lower in arid than in cold and humid regions. Thus, our outcomes also confirmed the findings of Atkinson et al. (2002), Goswami et al. (2007), Bai et al. (2015) and Zamoum and Souag-Gamane (2019), where the results in dry climate catchments were less accurate than those in humid climate catchments.

Concerning the climatic regionalization, we found a greater decrease in the model efficiency in the Tocsm catchments than in the Mpc catchments, where only a slight decrease was observed (Figure 7). The uncertainty in precipitation has a greater influence in wet catchments than in dry catchments, in agreement with the analysis by Pianosi and Wagener (2016).

To better understand the relationship between the decrease in model efficiencies relative to the calibration values when using regionalised parameters, the relationship of the GoF objective metric with the goodness of RegPar values has been analysed against the sensitivity of

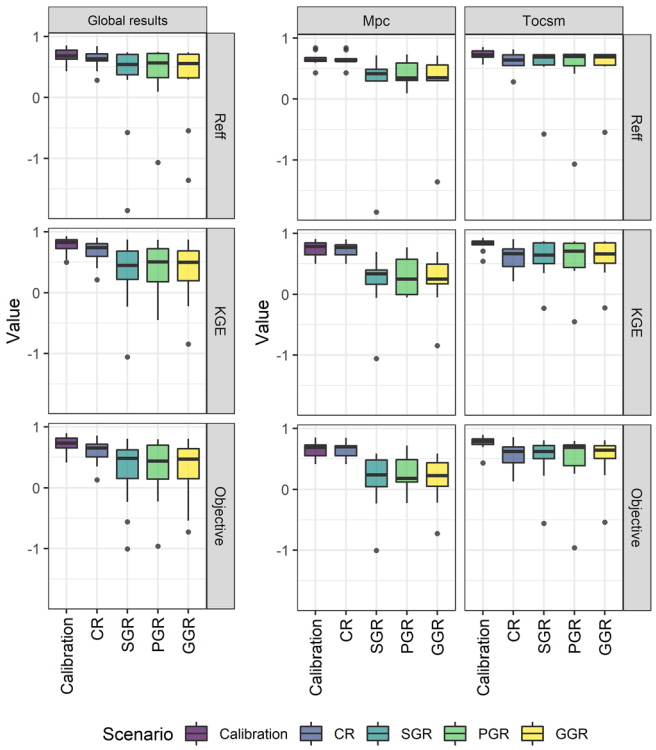

FIGURE 7 Boxplot graphic of the goodness of fit function values obtained in all the basins (global results on the left panel) and in both bioclimatic variants in the study area: the Mediterranean pluviseasonal-continental (Mpc) which is the driest variant, and temperate oceanic sub-Mediterranean (Tocsm) which is the most humid variant

the model to parameter errors. The results obtained (Figure SI.4) show how the drop in model efficiency is related to RegPar errors precisely when they occur in the most sensitive parameters of the model, with appreciable differences depending on the bioclimatic variants, as mentioned above. Therefore, it is worth noting that effectiveness in hydrological models highly depends on the climatic environment, and when comparing results with other studies, it is highly recommended to analyse the findings from the climatic rather than from the methodological point of view. This finding agrees with those reported by Yang et al. (2019) with respect to the greater influence of the regionalization method than climatological data in the evaluation of hydrological processes in areas with precipitation less than 3400 mm/year in Norway. In addition, although there are notable climatic differences between Norway and Spain, the same trend was observed in the present work, where the average annual rainfall was 1116 and 647 mm for the Tocsm and Mpc bioclimatic variants, respectively.

4.2.2 | Contribution of the spectral-based regionalization approach to the understanding of hydrological processes in ungauged catchments

Regarding our regionalized results on the ground parameters, the combined scenario, obtained by the combination of the spectral and physical attributes, did not improve the regionalization accuracies in any cluster, perhaps because the spectral response of the terrain is conditioned by the physical characteristics of the territory, and the sum of the predictors does not provide new information but, rather, redundant information to that provided by the RF algorithm.

Specifically, comparing the overall effectiveness for both bioclimatic variants together, of SGR versus PGR (Table 6), the median Reff value obtained in the SGR was slightly lower than the results of the PGR. These values agree with those reported by Merz and Blöschl (2004) in their best-regression-based scenario and with those reported by Götzinger and Bárdossy (2007) using a combined method (using the Lipschitz condition and a monotony condition) and those achieved by Jillo et al. (2017) in their regression-based study in Ethiopia. Finally, these values are better than those reported by Masih et al. (2010) in their flow-duration-curve-based regionalization approach. In contrast, our global results are worse than the results reported by Jin et al. (2009) in their proxy basin-based regionalization in a subtropical climate catchment. One of the main reasons could be the differences in climatic properties discussed below. At this point, we believe it is worth mentioning that none of the studies mentioned above used spectral data, except for Jillo et al. (2017), who used NDVI among other physical predictors.

On the other hand, if we analyse the results also considering the climatic differences, the results showed that in the driest catchments, the SGR outperformed the PGR scenario. In the Mpc catchments, the median Reff value was slightly better for the SGR than for the PGR, whereas in the Tocsm catchments, the median Reff values were similar for both scenarios. Considering this, the efficiencies of the SGR and PGR in the Tocsm catchments agree with those reported by Jin et al. (2009).

Regarding the PGR approach, we used the soil information from the European Soil Data Centre, which exhibited good performance. The results showed that soil information has a strong influence on the regression of parameters since topsoil properties are the most valuable predictors in the PGR and remain valuable predictors in the GGR, together with the texture-derived metrics from the SAR and NIR bands. The SGR showed better results than the PGR in the Mpc catchments, which are driest and characterized by medium to low vegetation coverage. This higher performance might be because the more valuable predictors in the SGR are mainly related to texture metrics for both SAR and optical bands. The SAR texture metrics are influenced by the grain size of the surface (Lu et al., 2021), and the radar capability for lithological analysis is better in sparse coverage than in dense vegetation areas (Radford et al., 2018). In addition, the optical information of the blue and NIR bands served as valuable predictors, as these latter bands were proven to be useful for geological applications in arid regions (Rajendran & Nasir, 2021). Moreover, regarding the VIs, the most valuable predictors in the RF classification are those that consider the noise of soil reflectance on vegetation in areas with sparse vegetation (MSAVI2, SAVI), especially MSAVI2, which also considers that different soils have different spectral responses (Qi et al., 1994). In addition, several VIs (GNDVI, MSAVI2, NDVI, and SAVI) and SI (CI) had a great influence

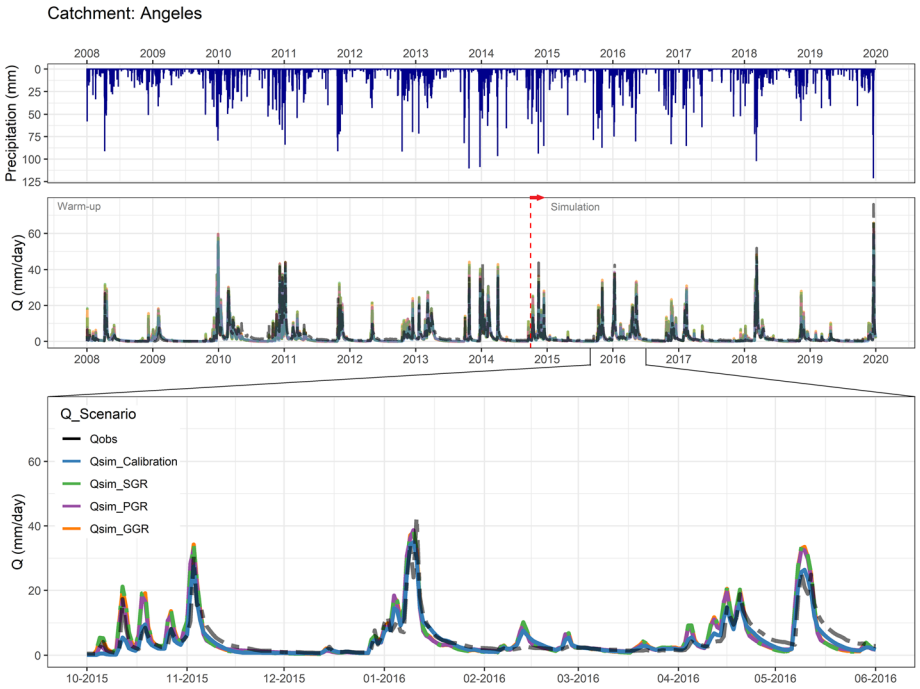

FIGURE 8 Observed and simulated streamflows in the scenarios for the calibration-validation periods at the Angeles catchment

TABLE 6 Summary of the GoF median values obtained in this work compared to the results obtained by other authors in previous works

	Calibration		Regionalisation				
			KGE		Reff (NSE)[a]		
	KGE	Reff (NSE)[a]	SGR[b]	PGR[b]	SGR[b]	PGR[b]	Study area
This work in the overall study area	0.83	0.68	0.45	0.5	0.54	0.57	Spain
This work in the driest climatic variant (Mpc)	0.78	0.64	0.33	0.25	0.42	0.35	Spain
This work in the most humid climatic variant (Tocsm)	0.84	0.73	0.64	0.71	0.69	0.70	Spain
Beck et al. (2020)	0.68	-	0.46		-		Global
	0.30[c]	-	−0.05		-		Arid
Alfieri et al. (2020)	0.61	0.35	-		-		Global
	0.82[d]	-	-		-		Europa
Masih et al. (2010)	-	-	-		0.47[e]		Iran
Merz and Blöschl (2004)	-	0.63	-		0.56		Austria
Jin et al. (2009)	-	0.78	-		0.72		China
Jillo et al. (2017)	0.63	-	0.5		-		Ethiopia
Oudin et al. (2008)	-	0.78	-		0.71–0.74		France
Götzinger and Bárdossy (2007)	-	0.53	-		0.50		Germany
Parajka et al. (2007)	-	0.66–0.69	-		-		Austria

Note: -, information not available or not analysed.
[a]Reff goodness of fit functions is also referred to as Nash-Sutcliffe efficiency (NSE).
[b]SGR, spectral ground regionalization; PGR, physical ground regionalization.
[c]Visual interpretation of fig. 5 in Beck et al. (2020) for arid climate class where Spain is located.
[d]Visual interpretation of fig. 6 in Alfieri et al. (2020).
[e]Estimated from table 7 in Masih et al. (2010) using the 7th best ranked.

on the estimation of the UZL parameter, which was one of the most sensitive parameters of the hydrological models and is involved in the percolation from the STZ towards the SUZ. Therefore, the SGR approach has been proven to be effective in analysing the relationship between the spectral response of the territory and its hydrological characteristics, allowing us to acquire a better understanding of both vegetation and top-upper-soil properties, especially in drier areas with sparse vegetation.

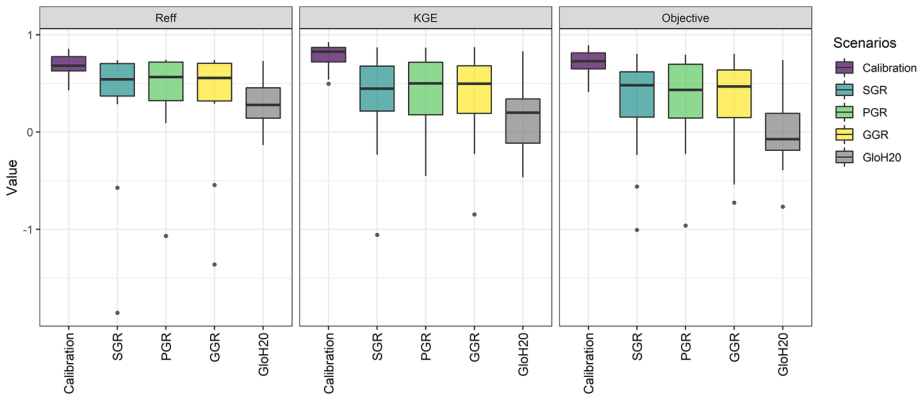

FIGURE 9 Performance of the GloH2O regionalized parameter dataset in the scenarios proposed in our work

4.2.3 | Is it worth performing a regional study when global databases exist?

We compared our regionalization effectiveness with the performance of the global high-resolution regionalized parameters (GloH2O) dataset developed by Beck et al. (2020). To this end, we processed the 10 cross-validation folds of available model parameters (BETA, FC, K0, K1, K2, LP, PERC, UZL, TT, CFMAX, CFR, and CWH) in the GloH2O dataset, and the ensemble-mean value was averaged in each catchment. For the parameters not mentioned above (PCALT, TCALT, SFCF, MAXBAS, and Cet), we assumed the Best-Par obtained in our calibration, and subsequently, the HBV models were run again for each catchment. Figure 9 shows that our regional approach outperformed the global GloH2O achievements in all GoFs analysed, and specifically the GoF reported in their study; our results (in terms of median values) for SGR (KGE = 0.45), PGR and GGR (both KGE = 0.50) outperformed the global GloH2O results (KGE = 0.20). Nevertheless, the latter value is in agreement with their own results for the arid climate class (into which our study area in Spain is classified, as shown in fig. 5 in Beck et al. (2020)), for which they reported a median KGE of approximately −0.05 for the calibration results (ranging from −0.20 in the 25th percentile to 0.15 in the 75th percentile). Therefore, given that in their global study, it appears that there are no study catchments in the Mediterranean area (see fig. 2 in Beck et al. (2020)), this finding would confirm that the GloH2O parameters in our study area achieved an effectiveness of approximately the same order of magnitude as those reported in the original study for arid climate classes. In addition, GloH2O achieved acceptable results in Tocsm and showed a median KGE value of approximately 0.28, whereas the results in Mpc were worse, at approximately −0.14. The main reason for these differences in the model efficiency may be the differences in the estimation of the most sensitive parameters in the catchments under study. It was observed that GloH2O overestimated the FC and UZL values and underestimated the K_0 values when compared to the Best-Par and Reg-Par obtained in our work (more details in Figure SI.5).

Hence, it is worth noting the importance of addressing regional studies where possible, particularly in drier climate variants, such as those of the Mediterranean environment, where the global model has been found to be less effective and where the spectral regionalization approach has achieved the best results.

4.3 | Uncertainties analysis

The main uncertainties in the streamflow simulations derive from the climatological data, from the time series gauging station stream flow records, from the structure of the HBV-light model itself and from the hydrological parameters involved in the analysis.

Regarding the climatological data, this study used precipitation and temperature data obtained through a statistical interpolation analysis of ground observation stations. The data were processed by the official meteorological agency in Spain, AEMET, guaranteeing the reliability of the data. However, the main limitation lies in the accuracy of the interpolation at the highest elevation, where there are usually no ground observation stations and the values are interpolated from records of ground stations located, generally, at lower elevations. To address this issue, the model parameters (PCALT and TCALT) were calibrated to ensure the balance of input and output volumes and minimize the error in volume. Then, a CR was proposed that considers the relative location of the ground observation stations and the catchments as predictors. Uncertainty related to CR, which mainly occurred in the wettest catchments, had a lesser impact on model efficiency than uncertainty related to GR.

The streamflow records used to validate the models, as mentioned above, correspond to an official source, that is, the SAIH of the hydrographic regions of Tajo and Guadiana in Spain. As an official data source, the SAIH is subject to an internal data validation process before publication, and as end users of the information, we do not have access to the raw data and validation; however, as the process is carried out by an official institution, a certain degree of accuracy is assumed. Furthermore, the information was rechecked by visual inspection.

Concerning the influence of the parameter values on the efficiency of the model, the impact on accuracy at the calibration stage was investigated by performing a sensitivity analysis. The overall trend is that the model showed greater sensitivity to the parameters related to the soil and top-upper zones of the groundwater routine (FC, UZL, and K0), and in the humid catchments, the PCALT was also sensitive.

In regard to HBV-light, the semidistributed approach was limited by the simplification of the three maximum allowed vegetation types, and considering this limitation, the land cover categories in the study area were grouped according to their runoff capability into three groups. In this sense, to make the models comparable, even though there was heterogeneity in land cover among the catchments, the same grouping criteria were applied to all of them.

4.4 | Future implications for the understanding of hydrological processes in the Mediterranean environment

Our results confirm that regionalization is still challenging in Mediterranean bioclimate variants, even where the new spectral approach SGR showed promising results. One of the key issues in the regionalization of hydrological parameters is the availability of attributes to be considered predictors (Merz & Blöschl, 2004) and their variability in nomenclature across regions or countries. Therefore, having continuous soil data throughout Europe, together with Sentinel information, offers us new opportunities in the regionalization of parameters at the European scale. As shown in Table SI.1, the previously studied sites are mainly concentrated in central and northern Europe, Austria (Merz & Blöschl, 2004; Parajka et al., 2007), Germany (Bárdossy, 2007; Götzinger & Bárdossy, 2007), and Iran (Masih et al., 2010), and there is a lack of studies on catchments in the Mediterranean environment. Future work could focus on regionalization in the Mediterranean area to complete the range of catchment typologies.

Moreover, Sentinel data offer continuous coverage throughout almost the entire world, offering new possibilities to study the hydrological processes in areas where cartographic information is not available. In addition, time series of satellite data could improve seasonal regionalization approaches characterizing the hydrologic response of the catchments and the seasonal variability that characterizes Mediterranean catchment flood events.

5 | CONCLUSIONS

In this study, the capability of a catchment's spectral signature for the regionalization of hydrological parameters was studied using a regression-based machine learning approach.

The calibration results were excellent (median KGE = 0.83), and regionalized parameters with the random forest algorithm achieved good performance. The general trend showed that the decrease in the efficiency relative to the calibration values was lower for the climate regionalization (variables related to precipitation, temperature and snow routine) (median KGE = 0.74) than for the ground regionalization (hydrological parameters involved in soil, groundwater, and routing routines). Specifically for the latter case, the three scenarios achieved almost the same performance: the new approach using the catchments' spectral signature from the Sentinel-1 and Sentinel-2 satellites (median KGE = 0.45), the traditional method using physical properties (data provided by the European Soil Data Centre) (median KGE = 0.50) and a fusion of spectral and physical properties (median KGE = 0.50). We found that the performance of the hydrological models highly depends on the climatic environment, and the prediction in catchments classified as temperate oceanic sub-Mediterranean (Tocsm) bioclimatic variants, the most humid variant, exhibited better performance than in those classified as the Mediterranean pluviseasonal-continental (Mpc), the driest variant. The physical approach, using the soil information from the European Soil Data Centre, exhibited good performance in general terms, and the spectral approach showed better results specifically in the driest catchments in the Mpc climatic variant. Herein, our results confirm that regionalization is still challenging in Mediterranean bioclimate variants, even where the new spectral approach showed promising results in predicting hydrological processes in ungauged catchments. Our proposed spectral-based regionalization and random forest approach has proven to be effective in analysing the relationship between the spectral response of the territory and its hydrological characteristics. The proposed method provides a better understanding of both vegetation and top-upper-soil properties, which, once the model uncertainties have been evaluated, have proven to be among the most sensitive parameters in hydrological forecasting.

Therefore, having continuous soil data throughout Europe, together with Sentinel information, offers us new opportunities in the regionalization of parameters at the European scale, especially to fill the gap in regionalization studies in the Mediterranean environment. Moreover, the continuous coverage of Sentinel data worldwide offers new possibilities in areas where cartographic information is unavailable. In addition, time series of satellite data can improve seasonal regionalization approaches characterizing the hydrologic processes of ungauged catchments and their seasonal variability.

ACKNOWLEDGEMENTS

This research was funded by the *Consejería de Economía, Ciencia y Agenda Digital* of *Junta de Extremadura* and the European Social Fund: A way of doing Europe, through the 'Financing of Predoctoral Contracts for the Training of Doctors in Public Research and Development Centers belonging to the Extremadura System of Science, Technology, and Innovation [file PD16018]'. This work was also supported by the *Consejería de Economía, Ciencia y Agenda Digital of Junta de Extremadura* (Spain) and co-funded by the European Regional Development Fund under Grants GR18052 (DESOSTE) and GR18028 (KRAKEN) as well as by *Universidad de Extremadura* under Grant 2021-1852X2-CONVENIO 025Ñ16. We thank *Confederación Hidrográfica del Guadiana* and *Tajo* for providing the river discharge series. We thank the AEMET for providing the climatic information. We thank the European Soil Data Centre (ESDAC) for providing the data about the topsoil physical properties for Europe and the European Soil Database v2.0. We thank the University of Zurich (Department of Geography) for providing us with a copy of the HBV-light software.

DATA AVAILABILITY STATEMENT

The random forest regression models developed in this study are available from the corresponding author upon reasonable request.

ORCID

Laura Fragoso-Campón https://orcid.org/0000-0003-0397-6247
Pablo Durán-Barroso https://orcid.org/0000-0003-1590-6924
Elia Quirós https://orcid.org/0000-0002-8429-045X

REFERENCES

AEMET. (2017). *Serie de precipitación diaria en rejilla con fines climáticos. Nota técnica 24 de AEMET*. https://www.aemet.es/es/conocermas/recursos_en_linea/publicaciones_y_estudios/publicaciones/detalles/NT_24_AEMET

AEMET. (2019). *Datos observacionales Precipitación y Temperatura*. http://www.aemet.es/es/serviciosclimaticos/cambio_climat/datos_diarios?w=2

Alfieri, L., Lorini, V., Hirpa, F. A., Harrigan, S., Zsoter, E., Prudhomme, C., & Salamon, P. (2020). A global streamflow reanalysis for 1980–2018. *Journal of Hydrology X*, *6*, 100049.

Allen, R. G., Pereira, L. S., Raes, D., & Smith, M. (1998). Chapter 3 – Meteorological data. In F.-F. a. A. O. o. t. U. Nations (Ed.), *Crop evapotranspiration – Guidelines for computing crop water requirements – FAO irrigation and drainage paper 56*. FAO – Food and Agriculture Organization of the United Nations.

Arsenault, R., & Brissette, F. (2016). Analysis of continuous streamflow regionalization methods within a virtual setting. *Hydrological Sciences Journal*, *61*(15), 2680–2693. https://doi.org/10.1080/02626667.2016.1154557

Atkinson, S. E., Woods, R. A., & Sivapalan, M. (2002). Climate and landscape controls on water balance model complexity over changing timescales. *Water Resources Research*, *38*(12), 50-1–50-17. https://doi.org/10.1029/2002WR001487

Bai, P., Liu, X., Liang, K., & Liu, C. (2015). Comparison of performance of twelve monthly water balance models in different climatic catchments of China. *Journal of Hydrology*, *529*, 1030–1040. https://doi.org/10.1016/j.jhydrol.2015.09.015

Ballabio, C., Panagos, P., & Monatanarella, L. (2016). Mapping topsoil physical properties at European scale using the LUCAS database. *Geoderma*, *261*, 110–123. https://doi.org/10.1016/j.geoderma.2015.07.006

Bárdossy, A. (2007). Calibration of hydrological model parameters for ungauged catchments. *Hydrology and Earth System Sciences*, *11*(2), 703–710. https://doi.org/10.5194/hess-11-703-2007

Beck, H. E., Pan, M., Lin, P., Seibert, J., van Dijk, A. I. J. M., & Wood, E. F. (2020). Global fully distributed parameter regionalization based on observed streamflow from 4,229 headwater catchments. *Journal of Geophysical Research: Atmospheres*, *125*(17), e2019JD031485. https://doi.org/10.1029/2019JD031485

Bergström, S. (1995). The HBV model. In V. P. Singh (Ed.), *Computer models of watershed hydrology*. (pp. 443–476) Water Resources Publications.

Betterle, A., Schirmer, M., & Botter, G. (2019). Flow dynamics at the continental scale: Streamflow correlation and hydrological similarity. *Hydrological Processes*, *33*(4), 627–646. https://doi.org/10.1002/hyp.13350

Booij, M. J. (2005). Impact of climate change on river flooding assessed with different spatial model resolutions. *Journal of hydrology*, *303*(1–4), 176–198. https://doi.org/10.1016/j.jhydrol.2004.07.013

Breiman, L. (2001). Random forests. *Machine Learning*, *45*(1), 5–32. https://doi.org/10.1023/A:1010933404324

Bui, Q.-T., Nguyen, Q.-H., Nguyen, X. L., Pham, V. D., Nguyen, H. D., & Pham, V.-M. (2020). Verification of novel integrations of swarm intelligence algorithms into deep learning neural network for flood susceptibility mapping. *Journal of Hydrology*, *581*, 124379. https://doi.org/10.1016/j.jhydrol.2019.124379

Buzacott, A. J. V., Tran, B., van Ogtrop, F. F., & Vervoort, R. W. (2019). Conceptual models and calibration performance—Investigating catchment bias. *Water*, *11*(11), 2424. https://doi.org/10.3390/w11112424

Chouaib, W., Alila, Y., & Caldwell, P. V. (2018). Parameter transferability within homogeneous regions and comparisons with predictions from a priori parameters in the eastern United States. *Journal of Hydrology*, *560*, 24–38. https://doi.org/10.1016/j.jhydrol.2018.03.018

Choubin, B., Solaimani, K., Rezanezhad, F., Roshan, M. H., Malekian, A., & Shamshirband, S. (2019). Streamflow regionalization using a similarity approach in ungauged basins: Application of the geo-environmental signatures in the Karkheh River basin, Iran. *Catena*, *182*, 104128. https://doi.org/10.1016/j.catena.2019.104128

Costa, S., Santos, V., Melo, D., & Santos, P. (2017). Evaluation of Landsat 8 and Sentinel-2A data on the correlation between geological mapping and NDVI. *Paper presented at the 2017 First IEEE international symposium of geoscience and remote sensing (GRSS-CHILE)*.

Crochemore, L., Isberg, K., Pimentel, R., Pineda, L., Hasan, A., & Arheimer, B. (2020). Lessons learnt from checking the quality of openly accessible river flow data worldwide. *Hydrological Sciences Journal*, *65*(5), 699–711. https://doi.org/10.1080/02626667.2019.1659509

Cui, Z., Huang, J., Tian, F., Gao, J., Wang, X., & Li, J. (2020). Quantifying the impacts of climate change and land use on hydrological processes: A comparison between mountain and lowland agricultural watersheds. *Hydrological Processes*, *34*, 5370–5383. https://doi.org/10.1002/hyp.13950

Devesa Alcaraz, J. A. (1995). *Vegetación y flora de extremadura*. Universitas Editorial.

European Space Agency. (2019). *Science Toolbox exploitation platform*. http://step.esa.int/main/toolboxes/snap/

Fragoso-Campón, L., Quirós, E., & Gutiérrez Gallego, J. A. (2020). Dehesa environment mapping with transference of a Random Forest classifier to neighboring ultra-high spatial resolution imagery at class and macro-class land cover levels. *Stochastic Environmental Research and Risk Assessment*, *1-32*, 2179–2210. https://doi.org/10.1007/s00477-020-01880-3

Fragoso-Campón, L., Quirós, E., & Gutiérrez Gallego, J. A. (2021). Optimization of land cover mapping through improvements in Sentinel-1 and Sentinel-2 image dimensionality and data mining feature selection for hydrological modeling. *Stochastic Environmental Research and Risk Assessment*, *35*, 2493–2519. https://doi.org/10.1007/s00477-021-02014-z

Fragoso-Campón, L., Quirós, E., Mora, J., Gutiérrez Gallego, J. A., & Durán-Barroso, P. (2020). Overstory-understory land cover mapping at the watershed scale: Accuracy enhancement by multitemporal remote sensing analysis and LiDAR. *Environmental Science and Pollution Research*, *27*(1), 75–88. https://doi.org/10.1007/s11356-019-04520-8

Godinho, S., Guiomar, N., & Gil, A. (2017). Estimating tree canopy cover percentage in a mediterranean silvopastoral systems using sentinel-2A imagery and the stochastic gradient boosting algorithm. *International Journal of Remote Sensing*, *1-23*, 4640–4662. https://doi.org/10.1080/01431161.2017.1399480

Goswami, M., O'Connor, K. M., & Bhattarai, K. P. (2007). Development of regionalization procedures using a multi-model approach for flow simulation in an ungauged catchment. *Journal of Hydrology*, *333*(2–4), 517–531.

Götzinger, J., & Bárdossy, A. (2007). Comparison of four regionalization methods for a distributed hydrological model. *Journal of Hydrology*, *333*(2–4), 374–384. https://doi.org/10.1016/j.jhydrol.2006.09.008

Guo, Y., Zhang, Y., Zhang, L., & Wang, Z. (2021). Regionalization of hydrological modeling for predicting streamflow in ungauged catchments: A comprehensive review. *Wiley Interdisciplinary Reviews: Water*, *8*(1), e1487. https://doi.org/10.1002/wat2.1487

Haralick, R. M., & Shanmugam, K. (1973). Textural features for image classification. *IEEE Transactions on Systems, Man, and Cybernetics*, *6*, 610–621. https://doi.org/10.1109/TSMC.1973.4309314

Hargreaves, G. H., Asce, F., & Allen, R. G. (2003). History and evaluation of Hargreaves evapotranspiration equation. *Journal of Irrigation and Drainage Engineering*, *129*(1), 53–63. https://doi.org/10.1061/(ASCE)0733-9437(2003)129:1(53)

He, Y., Bárdossy, A., & Zehe, E. (2011). A review of regionalisation for continuous streamflow simulation. *Hydrology and Earth System Sciences*, *15*(11), 3539–3553. https://doi.org/10.5194/hess-15-3539-2011

Hrachowitz, M., Savenije, H. H. G., Blöschl, G., McDonnell, J. J., Sivapalan, M., Pomeroy, J. W., Arheimer, B., Blume, T., Clark, M. P., Ehret, U., Fenicia, F., Freer, J. E., Gelfan, A., Gupta, H. V., Hughes, D., Hut, R., Montanari, A., Pande, S., Tetzlaff, D., & Cudennec, C. (2013). A decade of predictions in ungauged basins (PUB)—A review. *Hydrological Sciences Journal*, *58*(6), 1198–1255. https://doi.org/10.1080/02626667.2013.803183

Hundecha, Y., & Bárdossy, A. (2004). Modeling of the effect of land use changes on the runoff generation of a river basin through parameter regionalization of a watershed model. *Journal of Hydrology*, *292*(1–4), 281–295. https://doi.org/10.1016/j.jhydrol.2004.01.002

IGN. (2021). *Centro de Descargas*. Centro Nacional de Información Geográfica. http://centrodedescargas.cnig.es/CentroDescargas/index.jsp

Jayathilake, D. I., & Smith, T. (2019). Predicting the temporal transferability of model parameters through a hydrological signature analysis. *Frontiers of Earth Science*, *1-14*, 110–123. https://doi.org/10.1007/s11707-019-0755-y

Jillo, A. Y., Demissie, S. S., Viglione, A., Asfaw, D. H., & Sivapalan, M. (2017). Characterization of regional variability of seasonal water balance within Omo-Ghibe River basin, Ethiopia. *Hydrological Sciences Journal*, *62*(8), 1200–1215. https://doi.org/10.1080/02626667.2017.1313419

Jin, X., Xu, C.-y., Zhang, Q., & Chen, Y. D. (2009). Regionalization study of a conceptual hydrological model in Dongjiang basin, South China. *Quaternary International*, *208*(1–2), 129–137. https://doi.org/10.1016/j.quaint.2008.08.006

Joint Research Centre. (2020). *European Soil Data Centre (ESDAC)*. https://esdac.jrc.ec.europa.eu/

Kult, J. M., Fry, L. M., Gronewold, A. D., & Choi, W. (2014). Regionalization of hydrologic response in the Great Lakes basin: Considerations of temporal scales of analysis. *Journal of Hydrology*, *519*, 2224–2237. https://doi.org/10.1016/j.jhydrol.2014.09.083

Liaw, A., & Wiener, M. (2002). Classification and regression by randomForest. *R News*, 2/3.

Lu, Y., Yang, C., & Meng, Z. (2021). Lithology discrimination using Sentinel-1 dual-pol data and SRTM data. *Remote Sensing*, *13*(7), 1280. https://doi.org/10.3390/rs13071280

Ma, K., Feng, D., Lawson, K., Tsai, W.-P., Liang, C., Huang, X., Sharma, A., & Shen, C. (2021). Transferring hydrologic data across continents–leveraging data-rich regions to improve hydrologic prediction in data-sparse regions. *Water Resources Research*, *57*(5), e2020WR028600. https://doi.org/10.1029/2020WR028600

Masih, I., Uhlenbrook, S., Maskey, S., & Ahmad, M. D. (2010). Regionalization of a conceptual rainfall–runoff model based on similarity of the flow duration curve: A case study from the semi-arid Karkheh basin, Iran. *Journal of hydrology*, *391*(1–2), 188–201. https://doi.org/10.1016/j.jhydrol.2010.07.018

Merz, R., & Blöschl, G. (2004). Regionalisation of catchment model parameters. *Journal of Hydrology*, *287*(1–4), 95–123. https://doi.org/10.1016/j.jhydrol.2003.09.028

Oudin, L., Andreássian, V., Perrin, C., & Michel, C. (2008). Spatial proximity, physical similarity, regression and ungaged catchments: A comparison of regionalization approaches based on 913 French catchments. *Water Resources Research*, *44*, W03413. https://doi.org/10.1029/2007WR006240

Pagliero, L., Bouraoui, F., Diels, J., Willems, P., & McIntyre, N. (2019). Investigating regionalization techniques for large-scale hydrological modelling. *Journal of Hydrology*, *570*, 220–235. https://doi.org/10.1016/j.jhydrol.2018.12.071

Panagos, P. (2006). The European soil database. *GEO: Connexion*, *5*(7), 32–33.

Parajka, J., Viglione, A., Rogger, M., Salinas, J. L., Sivapalan, M., & Blöschl, G. (2013). Comparative assessment of predictions in ungauged basins – Part 1: Runoff-hydrograph studies. *Hydrology and Earth System Sciences*, *17*(5), 1783–1795. https://doi.org/10.5194/hess-17-1783-2013

Parajka, J., Blöschl, G., & Merz, R. (2007). Regional calibration of catchment models: Potential for ungauged catchments. *Water Resources Research*, *43*(6), W06406. https://doi.org/10.1029/2006WR005271

Parajuli, P. B., Jayakody, P., & Ouyang, Y. (2018). Evaluation of using remote sensing evapotranspiration data in SWAT. *Water resources management*, *32*(3), 985–996. https://doi.org/10.1007/s11269-017-1850-z

Pianosi, F., & Wagener, T. (2016). Understanding the time-varying importance of different uncertainty sources in hydrological modelling using global sensitivity analysis. *Hydrological Processes*, *30*(22), 3991–4003. https://doi.org/10.1002/hyp.10968

Prieto Sierra, C., Le Vine, N., Kavetski, D., García Alonso, E., & Medina Santamaría, R. (2019). Flow prediction in ungauged catchments using probabilistic random forests regionalization and new statistical adequacy tests. *Water Resources Research*, *55*, 4364–4392. https://doi.org/10.1029/2018WR023254

Purinton, B., & Bookhagen, B. (2020). Multiband (X, C, L) radar amplitude analysis for a mixed sand-and gravel-bed river in the eastern Central Andes. *Remote Sensing of Environment*, *246*, 111799. https://doi.org/10.1016/j.rse.2020.111799

Qi, J., Chehbouni, A., Huete, A. R., Kerr, Y. H., & Sorooshian, S. (1994). A modified soil adjusted vegetation index. *Remote Sensing of Environment*, *48*(2), 119–126. https://doi.org/10.1016/0034-4257(94)90134-1

Radford, D. D. G., Cracknell, M. J., Roach, M. J., & Cumming, G. V. (2018). Geological mapping in western Tasmania using radar and random forests. *IEEE Journal of Selected Topics in Applied Earth Observations and Remote Sensing*, *11*(9), 3075–3087. https://doi.org/10.1109/JSTARS.2018.2855207

Rajendran, S., & Nasir, S. (2021). ASTER mapping of gypsum deposits of Thumrait region of southern Oman. *Resource Geology*, *71*, 41–62. https://doi.org/10.1111/rge.12245

R-Core-Team. (2018). *R: A language and environment for statistical computing*. R Foundation for Statistical Computing. https://www.R-project.org/

Rivas-Martinez, S., & Rivas-Saenz, S. (1996-2019). *Worldwide bioclimatic classification system*. http://www.globalbioclimatics.org/form/tb_map/index.htm

Saadi, M., Oudin, L., & Ribstein, P. (2019). Random forest ability in regionalizing hourly hydrological model parameters. *Water*, *11*(8), 1540. https://doi.org/10.3390/w11081540

Seibert, J., & Vis, M. J. P. (2012). Teaching hydrological modeling with a user-friendly catchment-runoff-model software package. *Hydrology and Earth System Sciences*, *16*(9), 3315–3325. https://doi.org/10.5194/hess-16-3315-2012

Seibert, J. (1999). Regionalization of parameters for a conceptual rainfall-runoff model. *Agricultural and Forest Meteorology*, *98*, 279–293. https://doi.org/10.1016/S0168-1923(99)00105-7

Shen, C. (2018). A transdisciplinary review of deep learning research and its relevance for water resources scientists. *Water Resources Research*, *54*(11), 8558–8593. https://doi.org/10.1029/2018WR022643

Snelder, T. H., Lamouroux, N., Leathwick, J. R., Pella, H., Sauquet, E., & Shankar, U. (2009). Predictive mapping of the natural flow regimes of France. *Journal of Hydrology*, *373*(1–2), 57–67. https://doi.org/10.1016/j.jhydrol.2009.04.011

Swain, J. B., & Patra, K. C. (2019). Impact of catchment classification on streamflow regionalization in ungauged catchments. *SN Applied Sciences*, *1*(5), 1–14. https://doi.org/10.1007/s42452-019-0476-6

Tegegne, G., & Kim, Y.-O. (2018). Modelling ungauged catchments using the catchment runoff response similarity. *Journal of Hydrology*, *564*, 452–466. https://doi.org/10.1016/j.jhydrol.2018.07.042

Tyralis, H., Papacharalampous, G., & Langousis, A. (2019). A brief review of random forests for water scientists and practitioners and their recent history in water resources. *Water*, *11*(5), 910. https://doi.org/10.3390/w11050910

Ward, J. H., Jr. (1963). Hierarchical grouping to optimize an objective function. *Journal of the American Statistical Association*, *58*(301), 236–244. https://doi.org/10.1080/01621459.1963.10500845

Yang, X., Magnusson, J., & Xu, C.-Y. (2019). Transferability of regionalization methods under changing climate. *Journal of Hydrology*, *568*, 67–81. https://doi.org/10.1016/j.jhydrol.2018.10.030

Zamoum, S., & Souag-Gamane, D. (2019). Monthly streamflow estimation in ungauged catchments of northern Algeria using regionalization of conceptual model parameters. *Arabian Journal of Geosciences*, *12*(11), 1–14. https://doi.org/10.1007/s12517-019-4487-9

Zhang, Y., Chiew, F. H. S., Li, M., & Post, D. (2018). Predicting runoff signatures using regression and hydrological modeling approaches. *Water Resources Research*, *54*(10), 7859–7878. https://doi.org/10.1029/2018WR023325

SUPPORTING INFORMATION

Additional supporting information can be found online in the Supporting Information section at the end of this article.

How to cite this article: Fragoso-Campón, L., Durán-Barroso, P., & Quirós, E. (2022). Analysing the capability of a catchment's spectral signature to regionalize hydrological parameters. *Hydrological Processes*, *36*(8), e14673. https://doi.org/10.1002/hyp.14673